

PREPARED FOR SUBMISSION TO JCAP

Preprint: HIP-2015-6/TH

Inflationary Imprints on Dark Matter

Sami Nurmi,^{a,b} Tommi Tenkanen^a and Kimmo Tuominen^a

^aUniversity of Helsinki and Helsinki Institute of Physics,
P.O. Box 64, FI-00014, University of Helsinki, Finland

^bDepartment of Physics, University of Jyväskylä,
P.O. Box 35 (YFL), FI-40014 University of Jyväskylä, Finland

E-mail: sami.nurmi@helsinki.fi, tommi.tenkanen@helsinki.fi,
kimmo.i.tuominen@helsinki.fi

Abstract. We show that dark matter abundance and the inflationary scale H could be intimately related. Standard Model extensions with Higgs mediated couplings to new physics typically contain extra scalars displaced from vacuum during inflation. If their coupling to Standard Model is weak, they will not thermalize and may easily constitute too much dark matter reminiscent to the moduli problem. As an example we consider Standard Model extended by a Z_2 symmetric singlet s coupled to the Standard Model Higgs Φ via $\lambda\Phi^\dagger\Phi s^2$. Dark matter relic density is generated non-thermally for $\lambda \lesssim 10^{-7}$. We show that the dark matter yield crucially depends on the inflationary scale. For $H \sim 10^{10}$ GeV we find that the singlet self-coupling and mass should lie in the regime $\lambda_s \gtrsim 10^{-9}$ and $m_s \lesssim 50$ GeV to avoid dark matter overproduction.

Keywords: Dark matter, Inflation, Freeze-in, SM Higgs, Higgs portal

Contents

1	Introduction	1
2	Singlet dark matter and freeze-in without primordial condensates	2
3	Primordial condensates	3
3.1	Inflationary fluctuations and their evolution	3
3.2	The moduli problem	4
4	Freeze-in with the primordial condensates	5
4.1	Processes in the quartic regime	6
4.2	Processes in the quadratic regime	7
5	Estimating the total dark matter yield	7
5.1	Case I: The condensate decays completely	8
5.2	Case II: The condensate survives	9
6	Conclusions and outlook	11

1 Introduction

For the measured Higgs mass $m_h \simeq 125$ GeV the Standard Model (SM) vacuum is metastable up to remarkably high energies $\mu_c \sim 10^{11}$ GeV with a lifetime much longer than the age of the universe [1–4]. In the early universe the stability is crucially affected also by the large spacetime curvature. Radiative corrections to the Higgs potential necessarily induce the non-minimal curvature coupling $\xi\Phi^\dagger\Phi R$ which during inflation when $R \sim H^2$ may easily dominate the potential [5–7]. Indeed, it has been shown that if $\xi(\mu_{EW}) \gtrsim 0.1$ [5] at the electroweak scale the SM Higgs remains stable up to the highest inflationary scale $H_* \sim 10^{14}$ GeV consistent with the tensor bound [8, 9] without any need to include new physics.

New physics beyond SM is however implied by several cosmological observations, such as inflation itself, dark matter and baryon asymmetry. If the Higgs potential is not drastically modified by new physics the Higgs generically is a light and energetically subdominant field during inflation [5, 6, 10–17]. (The attracting possibility of Higgs-driven inflation requires a non-trivial deviation from the SM potential at high energies, such as a large coupling to spacetime curvature [18–23].) Inflationary fluctuations displace the light Higgs from its vacuum generating a primordial Higgs condensate [10, 11]. The resulting out-of-equilibrium initial conditions $h_* \sim H_*$ for the hot big bang epoch may have significant observational ramifications. Particle production from the time-dependent Higgs condensate may for example generate baryon asymmetry [24] or produce non-thermal dark matter [25]. A careful investigation of the observational effects is of key importance and could reveal powerful new tests of specific SM extensions at very high energy scales.

In this work we will investigate how the initial conditions set by inflation affect the generation of dark matter abundance in the interesting class of portal scenarios [26–28] where the SM fields feel new physics only through Higgs-mediated couplings. As a representative example we will consider a Z_2 symmetric scalar singlet s coupled to the Higgs field by

$V_{\text{int}} = \lambda_{\text{sh}}^2 \Phi^\dagger \Phi s^2$. This simplified example captures some interesting features of the portal models. The singlet constitutes a dark matter candidate [26, 27, 29, 30] and its dynamics at electroweak phase transition could allow for baryogenesis [31–33]. Analogously to Higgs also the singlet is generically a light field during inflation and gets displaced from vacuum [25]. In this simple setup the out-of-equilibrium initial conditions do not typically affect the electroweak baryogenesis as the scalar condensates have either decayed or diluted away by that time [25]. They could however significantly affect the dark matter abundance if the portal coupling is very weak $\lambda_{\text{sh}} \lesssim 10^{-7}$. In this case the singlet never thermalizes with the SM fields. The singlet dark matter originates entirely from non-thermal production of singlet particles through the so called freeze-in mechanism [27, 34–43]. As we will show in this paper, the presence of scalar condensates significantly alters the previous estimates for the efficiency of the process leading to novel interplay between dark matter properties and initial conditions sensitive to the inflationary scale. Moreover, the inflationary displacement of the singlet may also lead to overproduction of dark matter which places stringent constraints on viable singlet mass scales and the values of its self-coupling.

The paper is organized as follows: In Section 2 we define the Z_2 symmetric model and discuss the freeze-in mechanism of dark matter production. In Section 3 we discuss initial conditions set by inflation and the related moduli problem. In Section 4 we investigate the production of singlet dark matter through the freeze-in accounting for the presence of primordial scalar condensates in the Boltzmann equations. We then present our main results for the dark matter abundance and its dependence on scalar couplings and the inflationary scale in Section 5. Finally we summarize and discuss the results in Section 6.

2 Singlet dark matter and freeze-in without primordial condensates

We consider the SM extended to include a Z_2 symmetric scalar singlet [26, 29, 30]

$$V(\Phi, S) = m_h^2 \Phi^\dagger \Phi + \lambda_h (\Phi^\dagger \Phi)^2 + \frac{1}{2} m_s^2 s^2 + \frac{\lambda_s}{4} s^4 + \frac{\lambda_{\text{sh}}}{2} (\Phi^\dagger \Phi) s^2. \quad (2.1)$$

Here Φ is the Standard Model Higgs doublet and s is a real scalar singlet assumed to possess a Z_2 symmetry in order to make it stable. Therefore, the singlet constitutes a dark matter candidate. At low temperatures and in the unitary gauge, $\Phi = (0, (\nu + h)/\sqrt{2})^T$. We will assume that $m_s^2 > 0$ and $\lambda_{\text{sh}} > 0$, so there is no spontaneous symmetry breaking in the singlet sector. This guarantees that the singlet scalar is stable in the vacuum. Moreover, in the cases we will consider, the portal coupling λ_{sh} is assumed to be very weak. This guarantees that for light enough singlets there are no constraints from the invisible decay width of the Higgs at the LHC.

Usually the exact value of the self-interaction λ_s is considered to be irrelevant for dark matter abundance. However, as we shall see it is of uttermost importance in determining the initial conditions for low energy phenomena and, consequently, for the calculation of the total dark matter yield via the freeze-in mechanism relevant in the limit of weak portal coupling $\lambda_{\text{sh}} \lesssim 10^{-7}$.

To set the notation, we start with a brief review of the well-known freeze-in results [27, 34–43] obtained neglecting the impacts of primordial scalar condensates generated by inflation.

In the freeze-in setup the singlet dark matter is produced from the thermal bath of SM particles through out-of-equilibrium decays and scatterings. For concreteness, consider

the case where the dominant process is Higgs decay into two singlet particles [34] which is possible below T_{EW} whenever $m_h > 2m_s$. For a discussion of other Higgs mediated processes which for $m_h < 2m_s$ could also be important, see e.g. [35].

The evolution of number density of the singlet scalar is determined by the Boltzmann equation

$$\begin{aligned} \dot{n}_s + 3Hn_s = & \int d\Pi_h d\Pi_{s_1} d\Pi_{s_2} (2\pi)^4 \delta^4(p_h - p_{s_1} - p_{s_2}) \\ & \times (|\mathcal{M}|_{h \rightarrow ss}^2 f_h (1 + f_s)(1 + f_s) - |\mathcal{M}|_{ss \rightarrow h}^2 f_s f_s (1 + f_h)) , \end{aligned} \quad (2.2)$$

where $d\Pi_i = d^3k_i / ((2\pi)^3 2E_i)$, \mathcal{M} is the transition amplitude and f_i is the usual phase space density of particle i . The Higgs particles are assumed to be in thermal equilibrium, and in the usual approximation one assumes that Maxwell-Boltzmann statistics can be used instead of Bose-Einstein, $f_h \simeq e^{-E_h/T}$.

Setting $f_s = 0$ on the right hand side of Eq. (2.2) the singlet abundance, produced at low temperatures by thermal Higgs particles only, then becomes [34]

$$\Omega_s h^2 \approx 1.73 \times 10^{27} \frac{m_s \Gamma_{h \rightarrow ss}}{m_h^2} = 1.73 \times 10^{27} \frac{m_s}{m_h^2} \left(\frac{\lambda_{sh}^2 \nu^2}{32\pi m_h} \sqrt{1 - 4m_s^2/m_h^2} \right) . \quad (2.3)$$

In the limit, $m_s \ll m_h$, this yields a parametric estimate for the coupling sufficient to produce a sizeable dark matter abundance

$$\lambda_{sh} \simeq 10^{-11} \left(\frac{\Omega_s h^2}{0.12} \right)^{1/2} \left(\frac{\text{GeV}}{m_s} \right)^{1/2} . \quad (2.4)$$

The implied small coupling values are compatible with the key assumption of the freeze-in scenario that the dark matter candidate does not thermalize with the SM background above the EW scale.

The essential approximation in the above analysis, and commonly made in all freeze-in computations, is that the dark matter abundance is initially negligible, i.e. $f_s = 0$ on the right hand side of Eq. (2.2) [34, 35, 38]. However, this may not be the generic outcome in realistic setups where ramifications of the inflationary stage are consistently accounted for. Indeed, scalar dark matter candidates could easily get displaced from vacuum during inflation and their subsequent relaxation towards the low energy vacuum can significantly alter the freeze-in picture as we will now turn to discuss.

3 Primordial condensates

3.1 Inflationary fluctuations and their evolution

During inflation any energetically subdominant light scalar acquires superhorizon fluctuations proportional to the inflationary scale H_* . The spectators get locally displaced from their vacuum state and after the end of inflation the observable patch generically features primordial spectator condensates.

Within the extended SM (2.1) we are considering here, both the Higgs and the singlet are light spectators during inflation, $V'' \ll H^2$, and get displaced from vacuum [11, 25]. The typical amplitudes of the primordial Higgs and singlet condensates are given by the root mean square of fluctuations which for $\lambda_{sh} \lesssim \sqrt{\lambda_s \lambda_h}$ yields [44]

$$h_* = \mathcal{O}(0.1) \frac{H_*}{\lambda_h^{1/4}} , \quad s_* = \mathcal{O}(0.1) \frac{H_*}{\lambda_s^{1/4}} . \quad (3.1)$$

The inflationary scale H_* can be expressed in terms of the tensor to scalar ratio r and amplitude of the scalar perturbations \mathcal{P}_ζ as

$$\left(\frac{H_*}{2\pi}\right)^2 = \frac{r}{8}\mathcal{P}_\zeta. \quad (3.2)$$

In the following we adopt these generic order of magnitude estimates as the initial conditions for the hot big bang epoch and explore their impacts on the singlet dark matter yield.

Here we have assumed that the inflationary scale is below the flat space instability scale $H_* \lesssim 10^{11}$ GeV such that $\lambda(\mu) > 0$ and the curvature induced effective Higgs mass $\xi R h^2$ is negligible. If the inflationary scale is higher, one should carefully account for the non-minimal curvature coupling which dominates the Higgs dynamics when $\lambda \rightarrow 0$ [5, 6].

Assuming an efficient reheating of the SM sector soon after the end of inflation the Higgs condensate will be rapidly destroyed by the thermal bath [25] (see [11, 45, 46] for the decay at zero temperature and [47, 48] for reheating in the context of Higgs inflation). The singlet condensate on the other hand will not feel the thermal bath for $\lambda_{\text{sh}} \lesssim 10^{-7}$. Its evolution is affected by the redshifting due to expansion of space and also by out-of-equilibrium decays into singlet particles and Higgses through the portal coupling.

Neglecting the decay processes for the time being, the condensate stays nearly constant until $H^2 \sim \lambda_s s_*^2$ after which it starts to oscillate with a decreasing envelope

$$s_0(T) \simeq \begin{cases} 10^{-3} \lambda_s^{-3/8} r^{1/4} T, & T \gtrsim T_{\text{trans}} = 200 \lambda_s^{-1/8} r^{-1/4} m_s \\ 10^{-4} \lambda_s^{-5/16} r^{3/8} m_s^{-1/2} T^{3/2}, & T \lesssim T_{\text{trans}}. \end{cases} \quad (3.3)$$

For temperatures above T_{trans} the singlet sees an effectively quartic potential $\lambda_s s^4 \gg m_s s^2$ and its energy density scales as radiation, $\rho_s \propto a^{-4}$. Below T_{trans} the quadratic mass term takes over and the singlet energy density scales as non-relativistic matter, $\rho_s \propto a^{-3}$.

3.2 The moduli problem

If the weakly coupled singlet condensate enters the regime $\rho_s \sim a^{-3}$ before the matter-radiation equality its energy density may lead to overproduction of cold dark matter. This is essentially the well-known moduli problem encountered in a variety of different theories for early universe physics (see e.g. [49–51]).

In the SM extension by a scalar singlet (2.1) the moduli problem constrains the viable singlet mass scale m_s from above. Using (3.3) and requiring that the energy density of the singlet condensate at matter-radiation transition $T_{\text{eq}} \sim 0.8$ eV does not exceed the dark matter contribution $\Omega_s \lesssim \Omega_{\text{DM}}$ we obtain the mass bound

$$\frac{m_s}{\text{GeV}} \lesssim 10^{-5} \left(\frac{\lambda_s}{10^{-10}}\right)^{5/8} \left(\frac{r}{0.1}\right)^{-3/4}. \quad (3.4)$$

This constraint should be regarded as an absolute upper bound as it neglects the decay processes of condensate. The decays alleviate the constraint by causing the condensate amplitude to decrease faster and by depleting the singlet energy into the SM sector through Higgs mediated processes.

4 Freeze-in with the primordial condensates

The primordial singlet condensate will significantly alter the standard freeze-in picture [34, 35, 38]. Due to the time dependent background, singlet particles can be produced already well above the electroweak scale where $h = 0$. In this regime the effective Boltzmann equation for the number density of singlet particles takes the form

$$\begin{aligned} \dot{n}_s + 3Hn_s = & \int dPS_{s_0,s,h_1,h_2} |\mathcal{M}|_{h \rightarrow sh}^2 f_{s_0} f_h (1 + f_s)(1 + f_h) \\ & + \int dPS_{s_0,s_1,s_2,s_3} |\mathcal{M}|_{s \rightarrow ss}^2 f_{s_0} f_s (1 + f_s)(1 + f_s) \\ & - \int dPS_{s_0,s,h_1,h_2} |\mathcal{M}|_{s \rightarrow hh}^2 f_{s_0} f_s (1 + f_h)(1 + f_h) \\ & + \Gamma_{s_0 \rightarrow ss} n_{s_0} . \end{aligned} \quad (4.1)$$

Here $dPS_{s_0,a,b,c}$ denotes phase space measure for the condensate s_0 and particles a, b, c and contains the four-momentum conserving delta function. Furthermore n_{s_0} denotes the condensate number density,

$$n_{s_0} \equiv \int \frac{d^3k}{(2\pi)^3} f_{s_0} \equiv \frac{\rho_{s_0}}{m_{s,\text{eff}}} , \quad (4.2)$$

where the singlet effective mass is defined as $m_{s,\text{eff}}^2 = V''$. As the coherently oscillating background can only decay, inverse processes where particles would go back into the condensate are not present.

The amplitudes $M_{a \rightarrow bc}$ in (4.1) correspond to decay processes induced by the oscillating condensate and $\Gamma_{s_0 \rightarrow ss} n_{s_0}$ denotes the rate for particle production directly from the time dependent effective potential. We approximate the amplitudes by [52–54]

$$2\pi\delta^4(p_2 - p_1) \mathcal{M}_{1 \rightarrow 2} = \int_{-\infty}^{\infty} dt \langle 2|\hat{V}(t)|1 \rangle , \quad (4.3)$$

where $\hat{V}(t)$ denotes the interaction Hamiltonian induced by the singlet condensate¹. For example, in the case of $s \rightarrow h + h$ we have

$$\hat{V}(t) = -\lambda_{sh} s_0(t) \int d^3x \hat{s} \hat{h} \hat{h} . \quad (4.4)$$

To extract the leading contribution for the particle production induced by the condensate, we linearize the Boltzmann equation in f_h and f_s . After this the phase space integrals can be performed and (4.1) reduces to

$$\dot{n}_s + 3Hn_s \simeq \frac{K_1\left(\frac{m_h}{T}\right)}{K_2\left(\frac{m_h}{T}\right)} \Gamma_{h \rightarrow sh} n_h + \Gamma_{s_0 \rightarrow ss} n_{s_0} , \quad (4.5)$$

where K_n is the n th modified Bessel function of the 2nd kind. On the right hand side we have neglected the source terms related to the processes $s \rightarrow ss$ and $s \rightarrow hh$. These are

¹In the quartic regime, $\lambda_s s^4 \gg m_s s^2$, the system is conformal and the amplitude coincides with the Minkowski result. In the quadratic regime we keep using the Minkowski metric neglecting the small $\mathcal{O}(H/m_s)$ curvature corrections during one oscillation cycle.

suppressed by the small occupation numbers of singlet particles, $f_s \ll f_h, f_{s_0}$, and the latter are also kinematically heavily suppressed in the quartic regime.

The Boltzmann equation for particles (4.1) is accompanied by the corresponding equation of motion for the singlet condensate

$$\dot{n}_{s_0} + 3Hn_{s_0} = -(\Gamma_{s_0 \rightarrow ss} + \Gamma_{s_0 \rightarrow hh})n_{s_0} - \frac{K_1\left(\frac{m_h}{T}\right)}{K_2\left(\frac{m_h}{T}\right)}\Gamma_{h \rightarrow sh}n_h. \quad (4.6)$$

The three contributions on the right hand side correspond to energy loss due to production of singlet particles and Higgses out of the oscillating condensate. The decay processes have negligible effects on the condensate motion until $\Gamma \sim H$. Up to this point the background dynamics is therefore well described by the solution (3.3). As $\Gamma \sim H$ the amplitude of the condensate starts to decrease exponentially and to sufficient accuracy we can model the process as an instant decay at $\Gamma = H$. Consequently, the source terms in (4.5) vanish and the comoving singlet number density $a^3 n_s$ freezes to a constant. At the electroweak transition the generation of Higgs vacuum expectation value (vev) induces an additional contribution to the singlet number through the standard freeze-in mechanism.

4.1 Processes in the quartic regime

The decay rates in the Boltzmann equation take different values depending on whether the singlet is oscillating in the quartic $s_0 \gtrsim m_s/\sqrt{\lambda_s}$ or quadratic $s_0 \lesssim m_s/\sqrt{\lambda_s}$ regime of its potential. In terms of the temperature, these regimes correspond respectively to $T \gtrsim T_{\text{trans}}$ and $T \lesssim T_{\text{trans}}$, where the transition temperature is given by Eq. (3.3).

In the quartic regime $T \gtrsim T_{\text{trans}}$, the amplitude of the oscillating condensate scales as $s_0 \propto T$. The rate for the $h \rightarrow sh$ process in Eqs. (4.5) and (4.6) computed in the time-dependent background is given by

$$\Gamma_{h \rightarrow sh}^{(4)} = \frac{\lambda_{sh}^2}{24\pi} \sum_{n=1}^{\infty} \frac{|s_n|^2}{m_h} \frac{k_0}{E_{k_0}^h + E_{k_0}^s} \simeq 10^{-4} \lambda_s^{1/2} \lambda_{sh}^2 \frac{s_0^3}{T^2}. \quad (4.7)$$

Here k_0 is the final state momentum satisfying the energy conservation condition $E_{k_0}^h + E_{k_0}^s = m_h + n\omega$, where $\omega \simeq 0.489 m_{s,\text{eff}}$ is the oscillation frequency of the singlet condensate [55], and

$$s_0(t) = \sum_{n=-\infty}^{\infty} s_n e^{+i\omega n t}. \quad (4.8)$$

The other processes in Eqs. (4.5) and (4.6) correspond to transitions from vacuum to two singlet or two Higgs states, induced respectively by the interactions $\lambda_s s_0^2(t) s^2$ and $\lambda_{sh} s_0^2(t) h^2$. The corresponding rates are given by

$$\Gamma_{s_0 \rightarrow ss}^{(4)} = \frac{9\lambda_s^2}{16\pi} \frac{m_{s,\text{eff}}}{\rho_s} \sum_{n=1}^{\infty} |\zeta_n|^2 \sqrt{1 - \left(\frac{2m_{\delta s}}{n\phi}\right)^2} \simeq 4 \times 10^{-4} \lambda_s^{3/2} s_0 \quad (4.9)$$

$$\Gamma_{s_0 \rightarrow hh}^{(4)} = \frac{\lambda_{sh}^2}{16\pi} \frac{m_{s,\text{eff}}}{\rho_s} \sum_{n=1}^{\infty} |\zeta_n|^2 \sqrt{1 - \left(\frac{2m_h}{n\phi}\right)^2} \simeq 0, \quad (4.10)$$

where $m_{\delta s}^2 \equiv 3\lambda_s \langle s_0^2 \rangle$, and

$$s_0^2(t) - \langle s_0^2 \rangle = \sum_{n=-\infty}^{\infty} \zeta_n e^{-i\phi n t}, \quad (4.11)$$

with ϕ being the oscillation frequency of $\zeta(t)$. The rate (4.10) is negligible due to kinematical suppression by the thermal Higgs mass $m_h(T) \gg m_{s,\text{eff}}$.

4.2 Processes in the quadratic regime

In the quadratic regime the production of singlet particles directly from the time dependent background is energetically forbidden and consequently $\Gamma_{s_0 \rightarrow ss}^{(2)} = 0$. The transition $h \rightarrow sh$ induced by the time-dependent condensate is also kinematically blocked in this regime. The only possible process in Eqs. (4.5) and (4.6) is then the production of Higgses out of the time dependent background $s_0 \rightarrow hh$. The rate for this process is given by

$$\Gamma_{s_0 \rightarrow hh}^{(2)} = \frac{\lambda_{sh}^2 s_0^2}{64\pi m_s} \sqrt{1 - \left(\frac{m_h}{m_s}\right)^2}. \quad (4.12)$$

We reiterate that we are considering transitions in the time dependent background which amounts to the kinematical condition different for example from the standard $1 \rightarrow 2$ decay in vacuum.

From Eqs. (3.3) and (4.12) we obtain in the radiation dominated background the result

$$\frac{\Gamma_{s_0 \rightarrow hh}^{(2)}}{H} = \frac{\Gamma_{s_0 \rightarrow hh}^{(2)}}{H} \bigg|_{t_{\text{trans}}} \left(\frac{a_{\text{trans}}}{a} \right), \quad (4.13)$$

where t_{trans} denotes the time of transition from quartic to quadratic oscillations. Therefore, we immediately see that an eventual decay of the condensate needs to take place before the onset of quadratic oscillations. If the condensate has not decayed by t_{trans} the subsequent decay rates remain negligible and the condensate survives undecayed.

5 Estimating the total dark matter yield

The primordial singlet condensate crucially alters the standard freeze-in estimates for the abundance and properties of singlet dark matter. Depending on the strength of singlet self-coupling, the condensate may either completely decay into singlet particles or survive comprising a coherently oscillating dark matter component. The two cases could have different ramifications on structure formation, see e.g. [56–59]. The fate of the singlet condensate also affects the eventual decay channels of the singlet provided that the portal sector contains additional degrees of freedom such as fermions with Yukawa couplings $\mathcal{L} = g s \bar{\psi} \psi$.

In addition to the primordial condensates, singlet particles are produced at the electroweak transition through Higgs decays $\lambda_{sh} \nu h s s$. However, as opposed to the standard freeze-in estimates the singlet occupation numbers need not be small which could significantly affect the process. We leave a detailed analysis on this question to future work. In what follows we concentrate only on the abundance of singlet dark matter generated through the primordial condensates.

We also note that the observational bounds are significantly different depending on whether the singlet constitutes isocurvature or adiabatic dark matter. While the component sourced by the primordial condensates clearly is isocurvature, the situation is less clear when the production of singlet particles through Higgs decay is important. Any additional couplings between the SM and the portal sector would also affect the situation. We will not dwell further on this important issue but simply choose to present both the adiabatic and isocurvature bounds in what follows.

5.1 Case I: The condensate decays completely

As we have seen above, the condensate can decay only if the decay takes place in the quartic regime where $\lambda_s s_0^2 \gg m_s^2$. With the rates given in Eqs. (4.7), (4.9) and (4.10) the Boltzmann equations for the particles (4.5) and condensate (4.6) in this regime are given by

$$\dot{n}_s + 3Hn_s = \frac{K_1 \left(\frac{m_h}{T}\right)}{K_2 \left(\frac{m_h}{T}\right)} \Gamma_{h \rightarrow sh} n_h + \Gamma_{s_0 \rightarrow ss} n_{s_0} , \quad (5.1)$$

$$\dot{n}_{s_0} + 3Hn_{s_0} = -\frac{K_1 \left(\frac{m_h}{T}\right)}{K_2 \left(\frac{m_h}{T}\right)} \Gamma_{h \rightarrow sh} n_h - \Gamma_{s_0 \rightarrow ss} n_{s_0} . \quad (5.2)$$

Using that $n_{s_0} = \rho_s/m_{s,\text{eff}} = \lambda_s s_0^3/(4\sqrt{3})$ we can express the s_0 dependence of $\Gamma_{h \rightarrow sh}$ (4.7) in terms of n_{s_0} and rewrite the corresponding term in the condensate Boltzmann equation (5.2) as

$$\frac{K_1 \left(\frac{m_h}{T}\right)}{K_2 \left(\frac{m_h}{T}\right)} \Gamma_{h \rightarrow sh} n_h \simeq 10^{-4} \frac{K_1 \left(\frac{m_h}{T}\right)}{K_2 \left(\frac{m_h}{T}\right)} 4\sqrt{3} \lambda_{sh}^2 \frac{n_h}{T^2} n_{s_0} \equiv \tilde{\Gamma}_{h \rightarrow sh} n_{s_0} . \quad (5.3)$$

The solution for equation of motion (5.2) can then be written in the implicit form

$$n_{s_0} = n_{s_0, \text{osc}} \left(\frac{a_{\text{osc}}}{a} \right)^3 \exp \left(- \int_{a_{\text{osc}}}^a \frac{da}{a} \left(\frac{\Gamma_{s_0 \rightarrow ss}(s_0)}{H} + \frac{\tilde{\Gamma}_{h \rightarrow sh}}{H} \right) \right) , \quad (5.4)$$

where the quantities with subscript osc are evaluated at t_{osc} denoting the onset of quartic oscillations, $H_{\text{osc}} \sim \lambda_s s^2$ and only the first term inside the integral depends on n_{s_0} .

When $\Gamma_{s_0 \rightarrow ss}, \tilde{\Gamma}_{h \rightarrow sh} \lesssim H$ the particle production clearly has a negligible effect on the motion of the condensate. Using that² $\Gamma_{s_0 \rightarrow ss} \propto s_0$, and $\tilde{\Gamma}_{h \rightarrow sh} \propto T$ and substituting $s_0 \propto a^{-1}$ under the integral in Eq. (5.4) the integral can then be performed. This yields the approximative explicit solution

$$n_{s_0} \simeq 10^{-4} \frac{H_*^3}{\lambda_s^{1/4}} \left(\frac{a_{\text{osc}}}{a} \right)^3 \exp \left(- \frac{\Gamma_{s_0 \rightarrow ss}(s_0)}{H} - \frac{\tilde{\Gamma}_{h \rightarrow sh}}{H} \right) . \quad (5.5)$$

Here H_* denotes the inflationary Hubble rate at the horizon exit of observable modes.

For the weak portal couplings $\lambda_{sh} \lesssim 10^{-7}$ we are considering here, we generically have $\Gamma_{s_0 \rightarrow ss} \gg \tilde{\Gamma}_{h \rightarrow sh}$ if the condensate is to decay in the quartic regime. The decay time is then dictated by $\Gamma_{s_0 \rightarrow ss}$ and the condensate decays practically instantaneously at $H_{\text{dec}} = \Gamma_{s_0 \rightarrow ss}$ depleting all its energy into singlet particles. The solution of Boltzmann equation for singlet particles then reads

$$n_s \simeq \frac{1}{a^3} \left(\frac{K_1 \left(\frac{m_h}{T}\right)}{K_2 \left(\frac{m_h}{T}\right)} \Gamma_{h \rightarrow sh} n_h a^3 + n_{s_0} a^3 \right)_{t=t_{\text{osc}}} , \quad (5.6)$$

showing that the comoving number density freezes to a constant value as the time-dependent background vanishes. The behaviour is illustrated in Figure 1.

The distribution of the generated singlet particles is peaked at $k_*/a_{\text{dec}} \sim \sqrt{3\lambda_s} s_0$. As $\sqrt{3\lambda_s} s_0 > m_s$, after the decay of the condensate the produced singlet particles constitute

²See Eqs. (4.9), (5.3) and (3.3), respectively, for the following scalings.

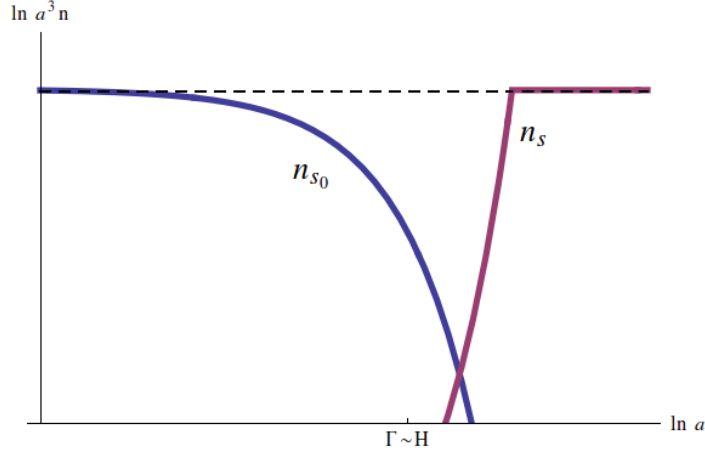


Figure 1. A schematic representation of the evolution of singlet number density and how it is divided between the condensate and excitations. The dashed line shows the constant comoving number density, the purple curve shows the number density of singlet particles and the blue one shows the number density of the condensate. The figure corresponds to the case where the interactions are sufficiently strong to allow for the condensate to decay away ($\Gamma \sim H$) before the quadratic part of the singlet potential starts to dominate the evolution (at T_{trans}). If the condensate survives until T_{trans} , it practically does not decay at all and its comoving number density remains almost constant.

effectively relativistic matter until $k_*/a \sim m_s$ and they become non-relativistic. If the decay of the condensate is complete, the corresponding transition temperature T_{trans} is given by Eq. (3.3) as before. For $T < T_{\text{trans}}$ the energy density of singlet particles is thus given by $\rho_s = m_s n_s$ which yields

$$\left(\frac{\Omega_s h^2}{0.12}\right) = 10^4 \lambda_s^{-7/4} \lambda_{\text{sh}}^2 \left(\frac{r}{0.1}\right)^{1/2} \left(\frac{m_s}{\text{GeV}}\right) + 10 \lambda_s^{-5/8} \left(\frac{r}{0.1}\right)^{3/4} \left(\frac{m_s}{\text{GeV}}\right). \quad (5.7)$$

for the present abundance of singlet dark matter.

The parametric dependence of the dark matter yield is illustrated in Figures 2 and 3. The red domain in the figures marks the regime where the condensate decays completely and dark matter consists of singlet particles. This domain exists only for sufficiently large values of the singlet self-coupling λ_s or the portal coupling λ_{sh} . For smaller couplings the condensate decay never becomes efficient and the final dark matter component will consist of the singlet condensate instead of particles.

As reviewed in Sec. 2, for superweak portal coupling the correct dark matter abundance can be generated at low temperature [27]. Here we have demonstrated that the primordial singlet condensate crucially affects the abundance and properties of singlet dark matter providing non-trivial boundary condition for the low temperature dark matter production. We leave for future work the careful matching of the low temperature particle production with the high temperature freeze-in we have described here.

5.2 Case II: The condensate survives

After the transition from quartic to quadratic oscillations the decay rate of the singlet condensate decreases faster than the Hubble rate. In the parameter range where $\Gamma_{s_0 \rightarrow ss} \ll H$

until the end of the quartic epoch the condensate therefore practically does not decay at all but is merely redshifted according to Eq. (3.3).

In more detail, the corresponding Boltzmann equation for singlet particles (4.5) in the quartic regime $T \gtrsim T_{\text{trans}}$ is given by,

$$\frac{dY_s^{(4)}}{dT} = -\frac{K_1 \left(\frac{m_h}{T}\right) \Gamma_{h \rightarrow sh}^{(4)}}{K_2 \left(\frac{m_h}{T}\right) H s_b T} n_h - \frac{\Gamma_{s_0 \rightarrow ss}^{(4)}}{H s_b T} n_{s_0} , \quad (5.8)$$

where $Y_s \equiv n_s/s_b$ denotes the singlet number density normalized by the entropy density of the bath s_b and where we used $\dot{T} \simeq -HT$, which is an excellent approximation above the EW scale. With the rates given in Eqs. (4.7), (4.9) and (4.10), the solution of Eq. (5.8) is

$$Y_s^{(4)}(T) = \left(4 \times 10^4 \lambda_{sh}^2 \lambda_s^{-5/8} \left(\frac{r}{0.1}\right)^{3/4} + 5 \times 10^2 \lambda_s^{1/2} \left(\frac{r}{0.1}\right) \right) \frac{\text{GeV}}{T}. \quad (5.9)$$

After the transition to the quadratic regime $T \lesssim T_{\text{trans}}$ the kinematical suppression renders the singlet particle production negligible and the comoving particle number freezes to a constant value. The corresponding present particle abundance is

$$\left(\frac{\Omega_s h^2}{0.12}\right) = 2.286 \times 10^9 \left(\frac{m_s}{\text{GeV}}\right) Y_s^{(4)}(T_0). \quad (5.10)$$

The final yield corresponding to the correct DM abundance today is depicted in Figures 2 and 3 for representative values of model parameters. The regions below the red domains correspond to the case where the condensate survives. The purple areas just over the blue regions depict the case II, where there is a small fraction of relic density also in the singlet particles. The dotted line denotes the upper bound for an isocurvature DM component, allowing only $\sim 1\%$ of non-thermally generated DM contributing to the observed total DM abundance [9]. The dashed lines, from thinnest to thickest denote 5%, 20%, 50% and 80% abundances, respectively. For example, in Figure 2 the upper boundary of the red region corresponds to 0.1% abundance and the lower boundary of the blue band to 100%. The yellow vertical band shows the standard freeze-in scenario [27, 34, 35], where only the low temperature processes ($h \rightarrow ss$) produce 1-100% of the present DM abundance, assuming $f_s = 0$ at $T = T_{\text{EW}}$. Note that the portal coupling is always required to be $\lambda_{sh} \lesssim 10^{-7}$ in order to avoid singlet thermalization before the electroweak scale.

As we have discussed above, one important consequence of the primordial singlet condensate is that it will lead to isocurvature perturbations which are heavily constrained by their imprints on the CMB anisotropies [9]. For the specific SM extension (2.1) we have concentrated on here, this constrains the singlet dark matter component to constitute at most only a very small fraction of the total dark matter abundance, as shown in Figures 2 and 3.

However, extending beyond the simplistic scenario (2.1) these constraints could be easily relaxed. In particular, we can entertain a thought that there are additional fields and interactions in the portal sector. These should not affect the high temperature evolution we have considered here, but could provide additional channels for the singlet sector to interact with the SM fields at temperatures below the electroweak transition. These interactions could convert the isocurvature modes into the observed adiabatic perturbations. A concrete possibility would be a superheavy scalar attaining a non-zero vev only at low temperatures.

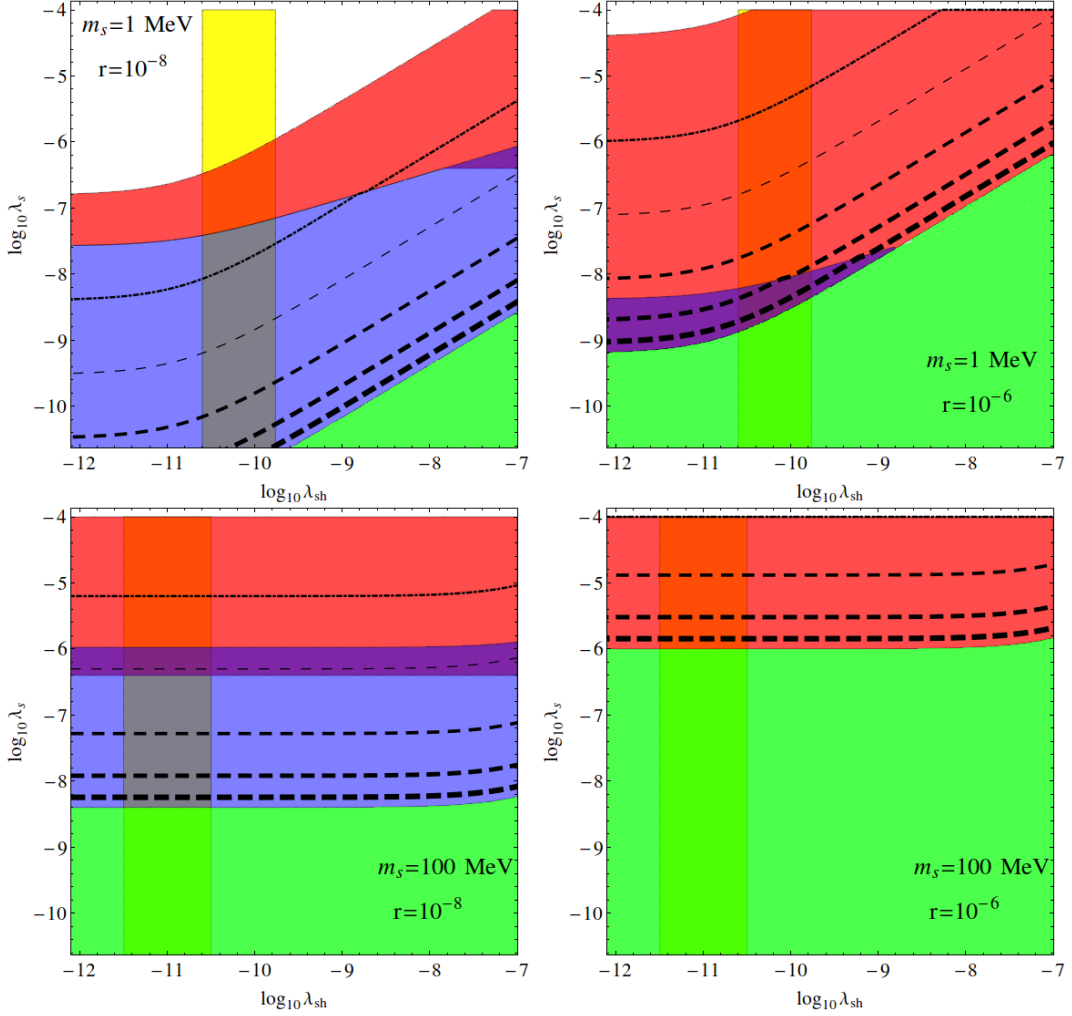


Figure 2. The final dark matter yield, shown in terms of the portal coupling λ_{sh} and the self-interaction coupling λ_s . Different regions where the model components (singlet condensate, singlet particles) produce 0.1-100% of today’s dark matter abundance are shown in red (particles only), blue (condensate only) and purple (both particles and condensate); see the main text for further explanations. The slashed contours refer to 80%, 50%, 20% and 5% abundances, listed from thickest to thinnest contour. The green region shows where the singlet would constitute more than 100% of today’s DM abundance. The dotted line denotes the upper bound ($\sim 1\%$) for an isocurvature DM component. The vertical yellow band shows the standard scenario where only the low temperature processes produce 1-100% of today’s DM abundance.

6 Conclusions and outlook

We have considered in detail the consequences of inflationary initial conditions on the dynamics of (extended) scalar sectors with light excitations. Concretely, we considered the simple benchmark model where the dark matter is constituted by a Z_2 symmetric real scalar field. Our main results are equations (5.7) and (5.10) together with Figures 2 and 3. They have strong implications on presently popular models of dark matter production via the freeze-in mechanism.

One particularly important feature we have uncovered is that, contrary to what is often

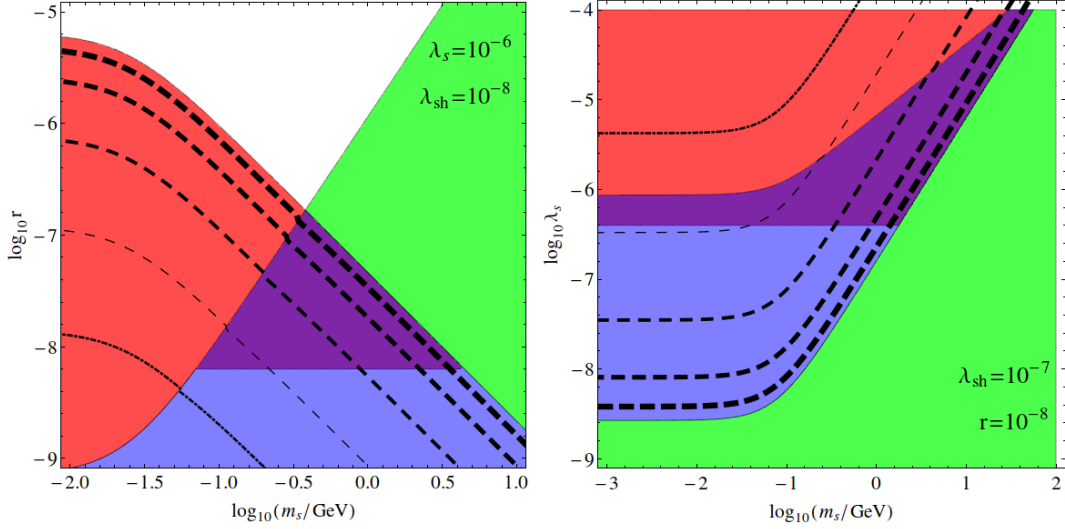


Figure 3. The final dark matter yield, shown in terms of the singlet mass m_s and tensor-to-scalar ratio r (left panel) or the self-interaction coupling λ_s (right panel). The different colours and contours are the same as in Figure 2.

assumed, λ_s is not irrelevant for the production of the dark matter abundance. Another important feature is that significant particle production via the freeze-in mechanism is possible at high-temperatures, above the electroweak scale, due to primordial condensates following from the initial conditions set by inflation. Consequently, the initial conditions for the singlet abundance to be negligible at $T \sim T_{\text{EW}}$ may not be valid. More generally, our analysis has revealed a novel connection how fundamental inflationary physics is imprinted on the dark matter abundance.³

Within the singlet scalar extension of SM we have shown how the freeze-in scenario severely constrains both the self-interaction coupling λ_s and portal coupling λ_{sh} . Our results can be also extended to provide new constraints on models in which the scalar acts only as a mediator and decays further to the actual DM particle such as a sterile neutrino. We will consider scenarios beyond the simple benchmark one treated in this paper in a forthcoming work.

Acknowledgements

We thank K. Kainulainen for discussions. This work was financially supported by the Academy of Finland projects 257532 (SN) and 267842 (KT). TT is supported by the Research Foundation of the University of Helsinki.

References

- [1] G. Degrassi, S. Di Vita, J. Elias-Miro, J. R. Espinosa, G. F. Giudice, et al., *Higgs mass and vacuum stability in the Standard Model at NNLO*, *JHEP* **1208** (2012) 098, [[arXiv:1205.6497](#)].
- [2] D. Buttazzo, G. Degrassi, P. P. Giardino, G. F. Giudice, F. Sala, A. Salvio, and A. Strumia, *Investigating the near-criticality of the Higgs boson*, *JHEP* **12** (2013) 089, [[arXiv:1307.3536](#)].

³For a related effect, see [[60](#)].

- [3] J. Ellis, J. R. Espinosa, G. F. Giudice, A. Hoecker, and A. Riotto, *The Probable Fate of the Standard Model*, *Phys. Lett.* **B679** (2009) 369–375, [[arXiv:0906.0954](#)].
- [4] O. Antipin, M. Gillioz, J. Krog, E. Mølgaard, and F. Sannino, *Standard Model Vacuum Stability and Weyl Consistency Conditions*, *JHEP* **1308** (2013) 034, [[arXiv:1306.3234](#)].
- [5] M. Herranen, T. Markkanen, S. Nurmi, and A. Rajantie, *Spacetime curvature and the Higgs stability during inflation*, *Phys.Rev.Lett.* **113** (2014), no. 21 211102, [[arXiv:1407.3141](#)].
- [6] J. Espinosa, G. Giudice, and A. Riotto, *Cosmological implications of the Higgs mass measurement*, *JCAP* **0805** (2008) 002, [[arXiv:0710.2484](#)].
- [7] M. Herranen, T. Markkanen, S. Nurmi, and A. Rajantie, *Spacetime curvature and Higgs stability after inflation*, [arXiv:1506.04065](#).
- [8] **BICEP2 Collaboration, Planck Collaboration** Collaboration, P. Ade et al., *A Joint Analysis of BICEP2/Keck Array and Planck Data*, *Phys.Rev.Lett.* (2015) [[arXiv:1502.00612](#)].
- [9] **Planck** Collaboration, P. Ade et al., *Planck 2015 results. XIII. Cosmological parameters*, [arXiv:1502.01589](#).
- [10] A. De Simone and A. Riotto, *Cosmological Perturbations from the Standard Model Higgs*, *JCAP* **1302** (2013) 014, [[arXiv:1208.1344](#)].
- [11] K. Enqvist, T. Meriniemi, and S. Nurmi, *Generation of the Higgs Condensate and Its Decay after Inflation*, *JCAP* **1310** (2013) 057, [[arXiv:1306.4511](#)].
- [12] K. Enqvist, T. Meriniemi, and S. Nurmi, *Higgs Dynamics during Inflation*, *JCAP* **1407** (2014) 025, [[arXiv:1404.3699](#)].
- [13] M. Fairbairn and R. Hogan, *Electroweak Vacuum Stability in light of BICEP2*, *Phys.Rev.Lett.* **112** (2014) 201801, [[arXiv:1403.6786](#)].
- [14] A. Kobakhidze and A. Spencer-Smith, *Electroweak Vacuum (In)Stability in an Inflationary Universe*, *Phys.Lett.* **B722** (2013) 130–134, [[arXiv:1301.2846](#)].
- [15] A. Hook, J. Kearney, B. Shakya, and K. M. Zurek, *Probable or Improbable Universe? Correlating Electroweak Vacuum Instability with the Scale of Inflation*, *JHEP* **1501** (2015) 061, [[arXiv:1404.5953](#)].
- [16] J. R. Espinosa, G. F. Giudice, E. Morgante, A. Riotto, L. Senatore, et al., *The cosmological Higgstory of the vacuum instability*, [arXiv:1505.04825](#).
- [17] J. Kearney, H. Yoo, and K. M. Zurek, *Is a Higgs Vacuum Instability Fatal for High-Scale Inflation?*, *Phys.Rev.* **D91** (2015) 123537, [[arXiv:1503.05193](#)].
- [18] F. L. Bezrukov and M. Shaposhnikov, *The Standard Model Higgs boson as the inflaton*, *Phys.Lett.* **B659** (2008) 703–706, [[arXiv:0710.3755](#)].
- [19] F. Bezrukov and M. Shaposhnikov, *Standard Model Higgs boson mass from inflation: Two loop analysis*, *JHEP* **0907** (2009) 089, [[arXiv:0904.1537](#)].
- [20] F. Bezrukov, A. Magnin, M. Shaposhnikov, and S. Sibiryakov, *Higgs inflation: consistency and generalisations*, *JHEP* **1101** (2011) 016, [[arXiv:1008.5157](#)].
- [21] F. Bezrukov, J. Rubio, and M. Shaposhnikov, *Living beyond the edge: Higgs inflation and vacuum metastability*, [arXiv:1412.3811](#).
- [22] F. Bezrukov and M. Shaposhnikov, *Higgs inflation at the critical point*, *Phys.Lett.* **B734** (2014) 249–254, [[arXiv:1403.6078](#)].
- [23] Y. Hamada, H. Kawai, K.-y. Oda, and S. C. Park, *Higgs Inflation is Still Alive after the Results from BICEP2*, *Phys.Rev.Lett.* **112** (2014), no. 24 241301, [[arXiv:1403.5043](#)].
- [24] A. Kusenko, L. Pearce, and L. Yang, *Postinflationary Higgs relaxation and the origin of matter-antimatter asymmetry*, [arXiv:1410.0722](#).

- [25] K. Enqvist, S. Nurmi, T. Tenkanen, and K. Tuominen, *Standard Model with a real singlet scalar and inflation*, *JCAP* **1408** (2014) 035, [[arXiv:1407.0659](#)].
- [26] J. McDonald, *Gauge singlet scalars as cold dark matter*, *Phys.Rev.* **D50** (1994) 3637–3649, [[hep-ph/0702143](#)].
- [27] J. McDonald, *Thermally generated gauge singlet scalars as selfinteracting dark matter*, *Phys.Rev.Lett.* **88** (2002) 091304, [[hep-ph/0106249](#)].
- [28] T. Alanne, K. Tuominen, and V. Vaskonen, *Strong phase transition, dark matter and vacuum stability from simple hidden sectors*, *Nucl.Phys.* **B889** (2014) 692–711, [[arXiv:1407.0688](#)].
- [29] C. Burgess, M. Pospelov, and T. ter Veldhuis, *The Minimal model of nonbaryonic dark matter: A Singlet scalar*, *Nucl.Phys.* **B619** (2001) 709–728, [[hep-ph/0011335](#)].
- [30] J. M. Cline, K. Kainulainen, P. Scott, and C. Weniger, *Update on scalar singlet dark matter*, *Phys.Rev.* **D88** (2013) 055025, [[arXiv:1306.4710](#)].
- [31] J. R. Espinosa, T. Konstandin, and F. Riva, *Strong Electroweak Phase Transitions in the Standard Model with a Singlet*, *Nucl.Phys.* **B854** (2012) 592–630, [[arXiv:1107.5441](#)].
- [32] S. Profumo, M. J. Ramsey-Musolf, and G. Shaughnessy, *Singlet Higgs phenomenology and the electroweak phase transition*, *JHEP* **0708** (2007) 010, [[arXiv:0705.2425](#)].
- [33] J. M. Cline and K. Kainulainen, *Electroweak baryogenesis and dark matter from a singlet Higgs*, *JCAP* **1301** (2013) 012, [[arXiv:1210.4196](#)].
- [34] L. J. Hall, K. Jedamzik, J. March-Russell, and S. M. West, *Freeze-In Production of FIMP Dark Matter*, *JHEP* **1003** (2010) 080, [[arXiv:0911.1120](#)].
- [35] C. E. Yaguna, *The Singlet Scalar as FIMP Dark Matter*, *JHEP* **1108** (2011) 060, [[arXiv:1105.1654](#)].
- [36] A. Merle, V. Niro, and D. Schmidt, *New Production Mechanism for keV Sterile Neutrino Dark Matter by Decays of Frozen-In Scalars*, *JCAP* **1403** (2014) 028, [[arXiv:1306.3996](#)].
- [37] M. Klasen and C. E. Yaguna, *Warm and cold fermionic dark matter via freeze-in*, *JCAP* **1311** (2013) 039, [[arXiv:1309.2777](#)].
- [38] M. Blennow, E. Fernandez-Martinez, and B. Zaldivar, *Freeze-in through portals*, [arXiv:1309.7348](#).
- [39] A. Adulpravitchai and M. A. Schmidt, *A Fresh Look at keV Sterile Neutrino Dark Matter from Frozen-In Scalars*, *JHEP* **1501** (2015) 006, [[arXiv:1409.4330](#)].
- [40] A. Merle and A. Schneider, *Production of Sterile Neutrino Dark Matter and the 3.5 keV line*, [arXiv:1409.6311](#).
- [41] F. Elahi, C. Kolda, and J. Unwin, *UltraViolet Freeze-in*, *JHEP* **03** (2015) 048, [[arXiv:1410.6157](#)].
- [42] A. Merle and M. Totzauer, *keV Sterile Neutrino Dark Matter from Singlet Scalar Decays: Basic Concepts and Subtle Features*, [arXiv:1502.01011](#).
- [43] Z. Kang, *View FIMP Miracle (by Scale Invariance) á la Self-interaction*, [arXiv:1505.06554](#).
- [44] A. A. Starobinsky and J. Yokoyama, *Equilibrium state of a selfinteracting scalar field in the De Sitter background*, *Phys.Rev.* **D50** (1994) 6357–6368, [[astro-ph/9407016](#)].
- [45] K. Enqvist, S. Nurmi, and S. Rusak, *Non-Abelian dynamics in the resonant decay of the Higgs after inflation*, *JCAP* **1410** (2014), no. 10 064, [[arXiv:1404.3631](#)].
- [46] D. G. Figueroa, J. Garcia-Bellido, and F. Torrenti, *The Decay of the Standard Model Higgs after Inflation*, [arXiv:1504.04600](#).

- [47] F. Bezrukov, D. Gorbunov, and M. Shaposhnikov, *On initial conditions for the Hot Big Bang*, *JCAP* **0906** (2009) 029, [[arXiv:0812.3622](#)].
- [48] J. Garcia-Bellido, D. G. Figueroa, and J. Rubio, *Preheating in the Standard Model with the Higgs-Inflaton coupled to gravity*, *Phys.Rev.* **D79** (2009) 063531, [[arXiv:0812.4624](#)].
- [49] G. Coughlan, W. Fischler, E. W. Kolb, S. Raby, and G. G. Ross, *Cosmological Problems for the Polonyi Potential*, *Phys.Lett.* **B131** (1983) 59.
- [50] T. Banks, M. Berkooz, S. Shenker, G. W. Moore, and P. Steinhardt, *Modular cosmology*, *Phys.Rev.* **D52** (1995) 3548–3562, [[hep-th/9503114](#)].
- [51] T. Banks, M. Berkooz, and P. Steinhardt, *The Cosmological moduli problem, supersymmetry breaking, and stability in postinflationary cosmology*, *Phys.Rev.* **D52** (1995) 705–716, [[hep-th/9501053](#)].
- [52] L. Abbott, E. Farhi, and M. B. Wise, *Particle Production in the New Inflationary Cosmology*, *Phys.Lett.* **B117** (1982) 29.
- [53] S. Weinberg, *The Quantum Theory of Fields volume I*. Cambridge University Press, 1995.
- [54] K. Ichikawa, T. Suyama, T. Takahashi, and M. Yamaguchi, *Primordial Curvature Fluctuation and Its Non-Gaussianity in Models with Modulated Reheating*, *Phys.Rev.* **D78** (2008) 063545, [[arXiv:0807.3988](#)].
- [55] P. B. Greene, L. Kofman, A. D. Linde, and A. A. Starobinsky, *Structure of resonance in preheating after inflation*, *Phys.Rev.* **D56** (1997) 6175–6192, [[hep-ph/9705347](#)].
- [56] W. Hu, *Structure formation with generalized dark matter*, *Astrophys.J.* **506** (1998) 485–494, [[astro-ph/9801234](#)].
- [57] W. Hu, R. Barkana, and A. Gruzinov, *Cold and fuzzy dark matter*, *Phys.Rev.Lett.* **85** (2000) 1158–1161, [[astro-ph/0003365](#)].
- [58] L. Amendola and R. Barbieri, *Dark matter from an ultra-light pseudo-Goldstone-boson*, *Phys.Lett.* **B642** (2006) 192–196, [[hep-ph/0509257](#)].
- [59] D. J. E. Marsh and J. Silk, *A Model For Halo Formation With Axion Mixed Dark Matter*, *Mon.Not.Roy.Astron.Soc.* **437** (2014), no. 3 2652–2663, [[arXiv:1307.1705](#)].
- [60] P. S. B. Dev, A. Mazumdar, and S. Qutub, *Connection between dark matter abundance and primordial tensor perturbations*, [arXiv:1412.3041](#).